Geologic controls on porosity development in the Maynardville Limestone, Oak Ridge, Tennessee

P. M. Goldstrand · L. A. Shevenell

Abstract Understanding the geologic controls of porosity development and their relationship to the karst aquifer system in the Cambrian Maynardville Limestone is important in determining possible contaminant transport pathways and provides essential data for hydrologic models within the Oak Ridge Reservation of east Tennessee. In the Maynardville Limestone, several important factors control porosity development: (1) lithologic controls on secondary microporosity and mesoporosity are related to dissolution of evaporite minerals and dedolomitization in supratidal facies; (2) depth below the ground surface controls the formation of karst features because the most active portion of the groundwater system is at shallow depths, and karst features are rare below ≈35 m; and (3) structural controls are related to solution enlargement of fractures and faults.

Key words Carbonate aquifer · Porosity · Karst

Introduction

The U.S. Department of Energy's Oak Ridge Y-12 Plant (Fig. 1), located in Bear Creek Valley (BCV) of east Tennessee, contains several hazardous and nonhazardous waste sites and underground storage tank sites within the valley and adjacent ridges that have the potential of contaminating local surface streams and groundwater. An understanding of porosity and karst development in this area is essential for proper flow characterization and for potential development of remedial alternatives. Because of the heterogeneous nature of the karst aquifer in BCV and its profound effects on contaminant transport, several hydrologic and geologic studies were conducted to help define groundwater pathways in BCV and to investigate the factors influencing the occurrence and distribution of water-bearing intervals. Results from drilling in BCV, core descriptions, diagenetic interpretations, and evaluation of secondary porosity development have been documented by Shevenell and others (1992), Goldstrand and Shevenell (1994), Goldstrand (1995), and Goldstrand and others (1995).

This paper defines the factors that result in secondary porosity development, both micro- and mesoporosity in the rock matrix, and macroporosity in the form of cavities. Cavities are important to this area because they allow rapid transmission of water and potential contaminants. Also, the matrix porosity, with its higher storage capacity, is important because it can act as a long-term source of contaminants. Contaminants can diffuse from the matrix porosity into cavities and fractures long after the primary source of the contaminants has been removed (e.g., Shevenell and others 1994). The objectives of this study are to help constrain the lithologic, structural, and spatial controls on porosity and karst development in this carbonate aquifer and to evaluate how these factors influence groundwater flow.

Received: 21 May 1996 · Accepted: 30 August 1996

P. M. Goldstrand (✉)
Geological Sciences Department, MS-172, University of Nevada, Reno, NV 89557, USA patrick@cs.unr.edu

L. A. Shevenell
Nevada Bureau of Mines and Geology, MS-178, University of Nevada, Reno, NV 89557, USA lisa@nbmg.unr.edu

General geology and hydrogeology

Geologic setting

Bear Creek Valley is located in the upper plate of the Whiteoak Mountain thrust fault (Fig. 1) within the Valley and Ridge province of the southern Appalachian fold and thrust belt, east Tennessee. The bedrock of BCV and adjacent ridges consists of Cambrian and Ordovician carbonate and clastic sedimentary rocks (King and Haase 1987; Hatcher and others 1992). The majority of the waste management areas within BCV are located in the uppermost part of the Conasauga Group (the Nolichucky Shale; Cn) and the lowermost part of the Knox Group (the Copper Ridge Dolomite; Ccr). Groundwater flows from the Ccr and the Cn into the Maynardville Limestone (Cmn) in the valley floor. Bedrock strike in the area varies locally from N47°E to N67°E and dips average 43° to the southeast (King and Haase 1987). The Cn forms the

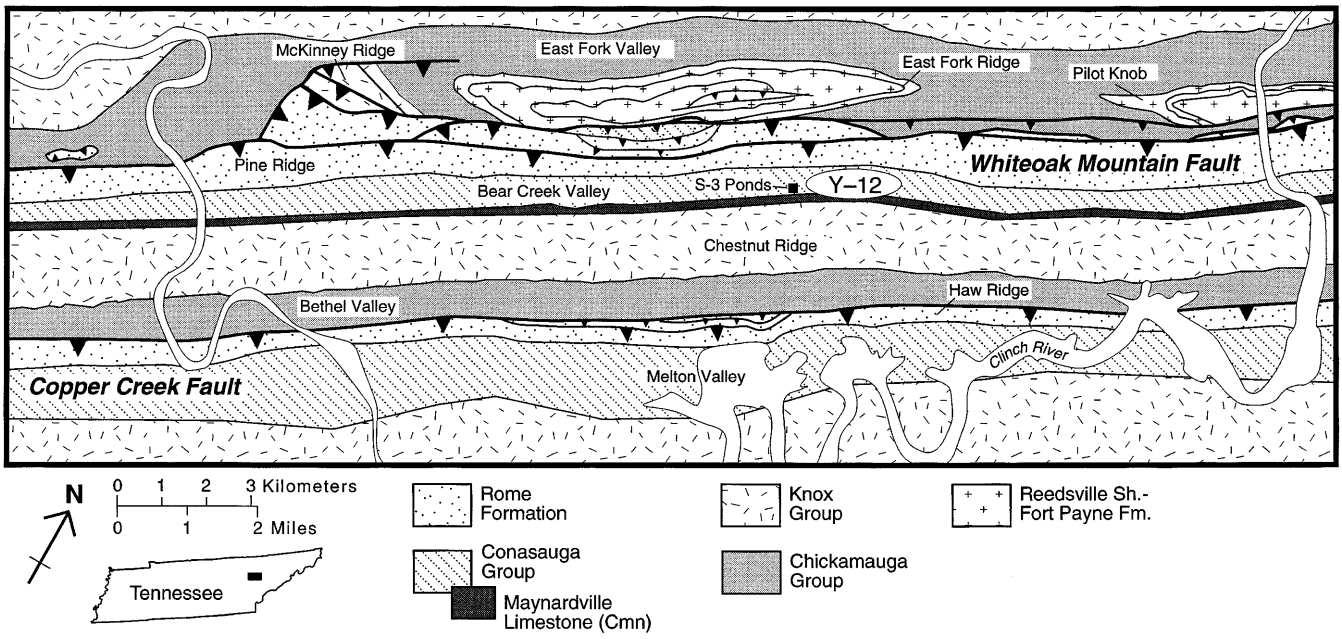

Fig. 1
Location and generalized geologic map for the Y-12 Plant area, Bear Creek Valley and Chestnut Ridge

central floor of BCV and is gradationally overlain by the Cmn. The Cmn forms the southeastern floor of BCV and is gradationally overlain by the ridge-forming Ccr, both of which are considered part of the Knox aquifer in this region (Solomon and others 1992).

The Cn ranges in stratigraphic thickness from 155 to 184 m in BCV (Hatcher and others 1992). The formation consists of massive to very thinly bedded shale intrastratified with thin- to medium-bedded limestone and rare calcareous siltstone. The interbedded shale and limestone of the upper Nolichucky Shale were deposited in a subtidal environment (Weber 1988; Foreman and others 1991).

The overlying Cmn ranges in stratigraphic thickness from 116 to 127 m in BCV (Hatcher and others 1992; Shevenell and others 1992). Based on gamma-ray log signatures, the uppermost Cn and the Cmn have been divided into six zones (Fig. 2). Zone 1 comprises the upper part of the Cn and is not part of this study. Zones 2–6 comprise the Cmn. On gamma-ray logs the contact between the Cn and Cmn is placed immediately above the highest right deflection (defining the location of the last major shale interbed within the Nolichucky Shale) and at the bottom of a comparatively constant carbonate baseline within the Cmn (Shevenell and others 1992). The Cmn-Ccr contact is gradational with mottled, irregularly bedded, dolomitic limestone within the uppermost Cmn grading upward into cherty dolostone of the Ccr.

Several fracture sets have been identified in the BCV area, with a prominent fracture set oriented parallel to and along bedding planes (Sledz and Huff 1981; Ketelle and Huff 1984; Rothschild and others 1984; Hatcher and others 1992). A second prominent set of fractures is also

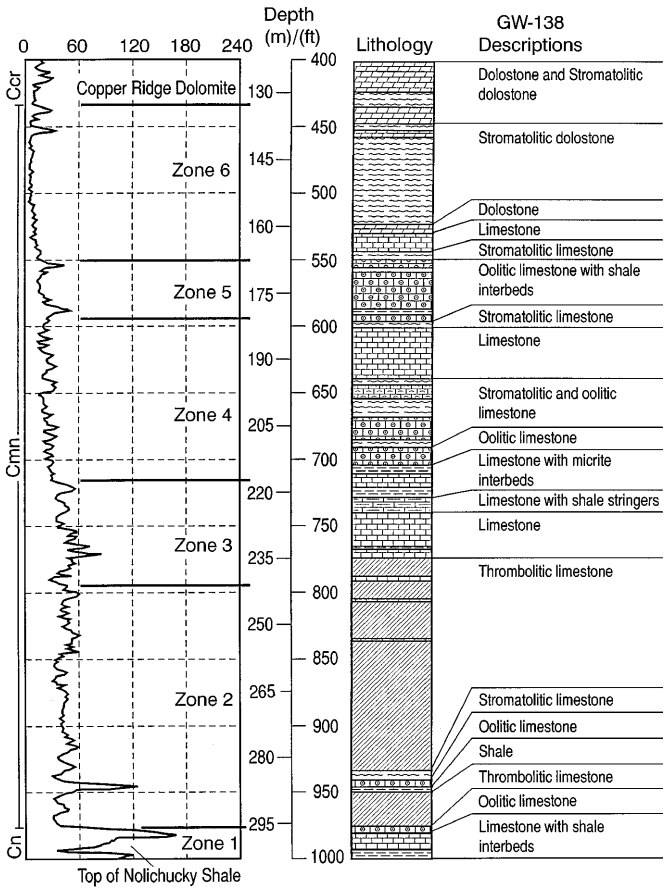

Fig. 2
Generalized natural gamma-ray log and lithologic column of Maynardville Limestone in Bear Creek Valley. Thickness shown is in down hole depth. All thicknesses in text are stratigraphic thicknesses

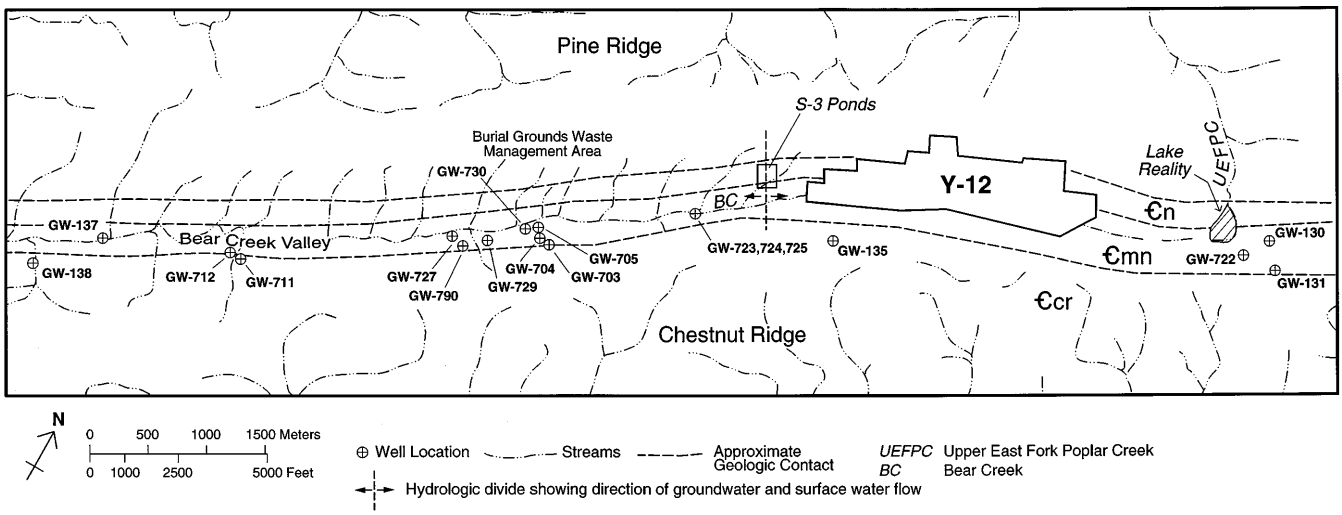

Fig. 3
Generalized map of Bear Creek Valley, Oak Ridge, Tennessee, showing borehole locations and approximate formation contacts for the Copper Ridge Dolomite (*Ccr*), Maynardville Limestone (*Cmn*), and Nolichucky Shale (*Cn*). Core descriptions, well logs, and geophysical data from boreholes shown were used for stratigraphic and sedimentologic correlations and interpretations. Core from wells GW-130, GW-135, GW-137, GW-138, and GW-722 were used for petrographic and porosity analysis

parallel to strike but perpendicular to bedding (Hatcher and others 1992). The frequency of fracturing decreases with depth below the ground surface (Solomon and others 1992). Also, there is a strong correlation between fracture spacing and bed thickness (i.e., wider fracture spacing in thicker beds; Hatcher and others 1992).
Although no major faults are present in the immediate study area, minor thrust faults (duplicating 3- to 6-m sections of strata) have been observed in core. These faults provide a zone of preferred groundwater flow paths and cavity development. Within the Burial Grounds area (Fig. 3) cavities (up to 1 m in vertical height) have developed along these fault planes. Grout, which was placed in cavities in one well during well completion attempts, was encountered in a second well located ≈ 50 m down dip within the fault zone, indicating these cavities are hydrologically connected along the fault plane.

Hydrogeologic setting

Hydraulic head data indicate groundwater flow into the Cmn is from the adjacent ridges through the Ccr and Cn in an approximately strike perpendicular direction. Flow in the Cmn is parallel to strike suggesting that the Cmn acts as a hydraulic drain for BCV. Within BCV a shallow groundwater and surface water divide is located near the southwest end of the Y-12 Plant in the area of the S-3 Ponds (Geraghty and Miller Inc. 1987; 1990; Fig. 3). Northeast of the divide, groundwater flows toward Upper East Fork Poplar Creek, and southwest of the divide the groundwater flow is southwest down Bear Creek (Fig. 3). The surface water in BCV and groundwater in the Cmn are interconnected, with springs discharging from the Cmn into Bear Creek (Geraghty and Miller Inc. 1985). A large number of solution cavities are present in the Cmn underlying Bear Creek (Shevenell and others 1992; Shevenell and Beauchamp 1994). Locally, intermittent rapid flow through these features occurs in response to precipitation events (Shevenell 1996).

Methods

Data pertaining to facies and lithologic variations within the Cmn were obtained from core and geophysical data from 18 boreholes throughout BCV (Goldstrand 1995). Eight lithofacies are identified from the Cmn and include: dolomitic limestone, dolostone, stromatolitic dolostone, stromatolitic limestone, oolitic limestone, limestone, thrombolitic limestone, and thinly interbedded limestone-shale lithofacies (Table 1). Petrographic analysis of 27 thin sections from wells GW-135, GW-137, and GW-138 (sample depths between 40 and 365 m) provides data on the mineralogy, porosity, and diagenetic evolution of the Cmn (Goldstrand 1995; Goldstrand and others 1995). Half of each thin section was stained for calcium carbonate and 300 points where counted per thin section. Volumetric porosity data were obtained from five coreholes (507 samples between 40 and 375 m depth) by the water immersion technique (Brown 1981) and are considered minimum porosity values (Goldstrand and others 1995). Note, core was not available from the shallower intervals (< 40 m).
The pore-size classification, used herein, is generally that defined by Choquette and Pray (1970) in which the diameter of micropores is < 0.0625 mm, small mesopores are between 0.0625 and 0.5 mm, large mesopores are between 0.5 and 4 mm, and megapores are 4–256 mm. Vuggy porosity (vugs) used in the context of this paper refers to roughly equant pores 1–5 cm in diameter. Cavities

Table 1
Percentage of lithofacies within each of the Maynardville Limestone geophysical zones. Data from 18 boreholes within Bear Creek Valley, east Tennessee

	Zone 6	Zone 5	Zone 4	Zone 3	Zone 2
Dolomitic limestone	13.95%	7.31%	5.20%	0.00%	0.07%
Dolostone	56.50%	1.79%	0.00%	0.00%	0.00%
Stromatolitic dolostone	11.54%	0.00%	0.00%	0.00%	0.00%
Stromatolitic limestone	1.38%	0.45%	11.79%	1.32%	1.06%
Oolitic limestone	3.53%	61.64%	28.50%	47.37%	1.92%
Limestone	13.09%	16.12%	37.52%	31.70%	11.76%
Thrombolitic limestone	0.00%	0.00%	15.74%	15.91%	83.15%
Interbedded limestone-shale	0.00%	12.69%	1.25%	3.71%	2.05%

(>6 cm) in the karst aquifer are considered to be macroporosity in this work.
Cavities are considered here as any solution-enlarged feature >6 cm in diameter and were identified during drilling of boreholes by noting an obvious drop in the drill string. Drops of several meters were noted in some wells, yet drops as small as 6 cm were also detected. These drops in the drill string only help to identify the vertical dimension of the cavity. In contrast, a fracture was identified during drilling by rig chatter, hematite and limonite staining on chip samples or core, and increased water production. An increase in water production which was not accompanied by hematite and limonite staining or rig chatter was considered to be a slower flowing water zone with groundwater flowing through the matrix microporosity and mesoporosity. In later discussions of cavity water zones versus other water zones, note that "other zones" refer to the combination of waters in fractures and matrix porosity.

Results

Lithologic observations

The Cmn is divided into five geophysically distinct zones numbered 2–6, with zone 2 at the base and zone 6 at the top of the formation (Fig. 2). Rapid facies changes are present within the lower part of the Cmn in BCV. Near the Burial Grounds Waste Management Area (Fig. 3), the stratigraphic thickness of zone 2 varies by ≈60 m over a horizontal distance of ≈110 m (Goldstrand 1995). This zone is dominantly composed of very fine to finely crystalline thrombolitic (nonlaminated algal) limestone (Table 1), with abundant thin, wispy shale and carbonate mudstone stringers and partings. Beds are massive to thickly bedded boundstone, packstone, and grainstone. Interbeds of bioclastic, peloidal, oolitic, stromatolitic, and oncolitic limestone are common. Zone 2 is commonly stylolitic and burrowed, and open and calcite-filled vugs and fractures are common. Locally, pyrite is either associated with shale stringers or is dispersed throughout the thrombolitic limestone.
Zone 3, as well as zone 2, thins and in places is absent near the Burial Grounds Waste Management Area. The base of zone 3 is gradational with zone 2 and interbeds of thrombolitic and oolitic limestone, matrix-supported carbonate conglomerate, carbonate mudstone, and stringers of calcareous shale are common. Interbeds of peloidal and oncolitic packstone and grainstone are common. The upper parts of zone 3 consist of oncolitic and oolitic limestone, thick interbeds of digitate stromatolitic limestone and slightly dolomitic mudstone. Black shale interbeds and stringers are more common within the peloidal and oolitic limestone beds.
Zone 4 consists of medium to coarsely crystalline limestone and minor dolostone. Interbeds of oolitic, digitate stromatolitic, and algal laminated limestones occur near the base. Interbeds of oncolitic limestone and dolomitic limestone occur in the upper part of this zone. Stromatolitic and bioclastic limestone beds are common. Calcite-filled birds-eye structures and gypsum- and anhydrite-filled vugs are also present in deeper core. Generally, zone 4 thins and grades into thrombolitic and stromatolitic limestone with interbeds of oolitic limestone in the Burial Grounds Waste Management area, and thickens to the northeast and southwest.
Zone 5 consists mostly of thickly bedded, oolitic, peloidal, and oncolitic limestone and dolomitic limestone. Laterally persistent, very thin interbeds and stringers of calcareous shale and micrite are characteristic of this zone. Thin intraformational conglomerate beds are also associated with the shale and micrite beds.
Zone 6 consists dominantly of dolostone and slightly calcareous dolostone (Table 1). Generally, this zone is medium to coarsely crystalline with a saccharoidal texture, massive to well-laminated, and stromatolitic. Rip-up clasts of algal laminated dolostone, bioturbation, and birds-eye structures are common. Stylolites, open and filled (calcite and gypsum) vugs and veins are common. An abundance of vugs and small (cm-scale) cavities is characteristic of this zone.
The Cmn represents an upward shallowing carbonate platform sequence from subtidal (zone 2) to supratidal (zone 6) paleoenvironments (Weber 1988; Goldstrand 1995). Rapid facies changes occurred in the subtidal portion of this carbonate platform (i.e., zones 2, 3, and 4) in

the area of the Burial Grounds. However, facies in zone 6, and to a lesser extent in zone 5, are generally uniform throughout BCV.

Lithologic controls on porosity development

Following the definitions of Choquette and Pray (1970), primary porosity is considered to be that porosity present in the rock after final deposition and secondary porosity is any post-depositional porosity created within the rock. Petrographic analysis indicates all primary porosity has been occluded through cementation and that all of the porosity present in the Cmn at this time is secondary or post-depositional in origin.

Volumetric porosity data provide an estimate of the microporosity and small mesoporosity for the Cmn zones (Table 2). Core inspection and petrographic analysis provided the most important clues on the controls of smaller-scale secondary porosity (microporosity to vugs). The major controls on the development of porosity are, in order of importance: (1) dissolution of gypsum and anhydrite, (2) dedolomitization, (3) carbonate grain size, and (4) oxidation and dissolution of pyrite.

Dissolution of gypsum and anhydrite nodules is responsible for the development of vuggy porosity within the supratidal part of the Cmn (zone 6). Nodules of gypsum and anhydrite are preserved in deeper core in the Cmn (e.g., well GW-135; 359 m depth) suggesting that dissolution is partly depth dependent. At shallow depths, vugs the size and shape of these nodules are lined with euhedral calcite crystals, suggesting dissolution of the evaporite minerals and later precipitation of calcite within the void (Saunders and Toran 1994; Goldstrand 1995). Petrographic analysis of vugs partially filled with gypsum from well GW-722 at 159 m depth indicates partial dissolution of the gypsum had occurred but that later precipitation of calcite has occluded some of that secondary porosity.

Dedolomitization (replacement of dolomite by calcite) is chemically related to the dissolution of gypsum within the Cmn and Ccr (Saunders and Toran 1994) and is an important factor in microporosity and mesoporosity development in the dolomitic parts of this formation (Goldstrand 1995). Ferroan dolomite is abundant throughout the upper Cmn, and relatively common throughout the middle and lower Cmn. The ferroan dolomite may have developed during burial diagenesis, replacing original fine-grained carbonate lithologies. In core, generally shallower than 180 m below ground surface (bgs), ferroan dolomite has been preferentially dissolved with respect to the surrounding carbonate lithologies. In some cases, replacement by calcite pseudomorphs after dolomite has occurred, but generally dissolution of the dolomite crystals has produced moldic micropores and mesopores.

Carbonate mud dissolution in the thrombolitic limestone facies, abundant in zones 2, 3 and 4, is an important process in the formation of secondary porosity in these zones. Similar results have been observed in other studies (Rauch and White 1970; Dreiss 1984), which indicate that smaller carbonate grain-sizes provide a larger surface area for active dissolution by groundwater undersaturated with $CaCO_3$.

Locally, dissolution of pyrite is also responsible for the development of secondary porosity. The transformation involves the oxidation of pyrite to hematite and ultimately the formation of moldic porosity with removal of the hematite. This form of porosity is generally restricted to thrombolitic limestone facies within zone 2 at depths less than 60 m.

Matrix porosity data from BCV indicate that porosities in the Cmn are in part lithologically and facies dependent. Below is a summary of the porosity development in each of the Cmn geophysical zones.

Zone 2: Within zone 2, a large number of vugs, as deep as 366 m bgs, are present, but the mean matrix porosity is 0.5%. Much of zone 2 consists of thrombolitic limestone, with dissolution concentrated in the intercalated micrite or along the wispy carbonate mud stringers (creating thin, elongate solution zones). Elongate solution zones also occur along the interface between shale stringers and carbonate lithologies, and are related to dissolution as groundwater moves along the shale-carbonate interface. These stratabound alteration zones account for localized higher porosities up to 4.0% (e.g., GW-130 at 92 m). At depths <60 m oxidation of pyrite to hematite was observed in zone 2. Complete alteration of the pyrite and removal of the hematite has produced moldic porosities as high as 3.0%.

Zone 3: Porosities in zone 3 range between 0.1 and 2.7%, with a mean matrix porosity of 0.6%. Porosity is associated with thrombolitic interbeds in which the intervening carbonate mudstones have dissolved.

Table 2
Mean matrix porosities for the Maynardville Limestone

Formation/ zone	Maximum–Minimum	Mean	Standard deviation	Number of samples
Zone 6	10.3–0.3%	2.1%	2.0	66
Zone 5	2.3–0.2%	0.8%	0.6	42
Zone 4	1.1–0.1%	0.5%	0.2	105
Zone 3	2.7–0.1%	0.6%	0.5	75
Zone 2	4.0–0.1%	0.5%	0.5	219
Total		0.8%		507

Zone 4: Zone 4 has a mean matrix porosity of 0.5% with porosity values ranging from 0.1 to 1.1%. Vuggy and moldic porosity within zone 4 occurs mostly in stromatolitic dolomitic limestones and is related to dedolomitization (see zone 6 below).
Zone 5: Matrix porosities for zone 5 range between 0.2% and 2.3%, with a mean porosity of 0.8%. This zone consists generally of coarsely crystalline, oolitic dolomitic limestone with interbeds of shale and micrite. The development of moldic porosity in this zone is related to the dissolution of dolomite crystals that commonly replace ooids (dedolomitization). Dissolution of micrite interbeds is also common.
Zone 6: The mean matrix porosity of zone 6 is 2.1%, but porosities locally exceed 10% (well GW-135 at a depth of ≈234 m). Vuggy porosity is abundant in zone 6 to a depth of 244 m bgs. Lithologically, zone 6 consists mostly of stromatolitic dolostone and calcareous dolostone. The highest porosities are present within the stromatolitic dolostone (Fig. 4). The predominant cause for the vuggy porosity in this zone is the dissolution of gypsum nodules (leaving abundant vugs up to several centimeters in diameter). Also of importance to the development of secondary porosity is dedolomitization. Selective dissolution of dolomite crystals has created abundant, interconnected moldic micropores and small mesopores (generally less than 0.5 mm in diameter). The processes of gypsum dissolution and dedolomitization are geochemically related (Back and others 1983; Saunders and Toran 1994) and are the major cause of porosity development in this zone. Porosity has also developed due to dissolution of carbonate mud within the dolomite. The stromatolitic dolomites are coarsely crystalline with intercalated carbonate mud laminae, which originally were trapped between the algal structures and filaments responsible for forming the stromatolites. Dissolution of the intervening carbonate mud produces elongate vugs several millimeters in diameter.

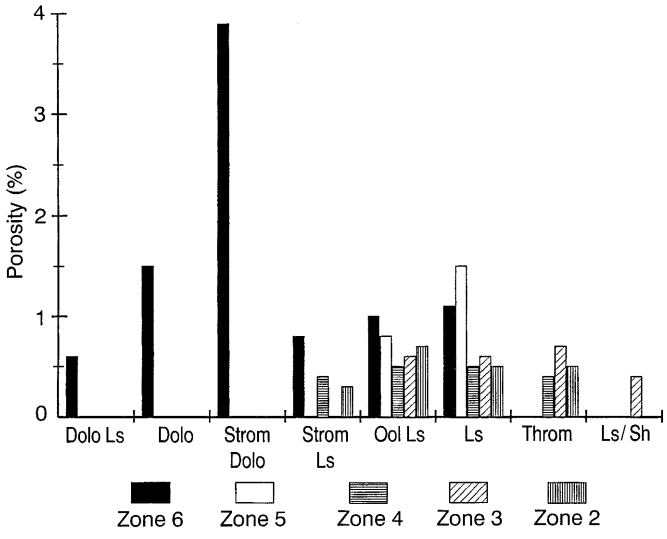

Fig. 4
Mean matrix porosities for Maynardville Limestone lithofacies and geophysical zones. Lithofacies: *Dolo Ls* dolomitic limestone, *Dolo* dolostone, *Strom Dolo* stromatolitic dolostone, *Strom Ls* stromatolitic limestone, *Ool Ls* oolitic limestone, *Ls* limestone, *Throm* thrombolitic limestone, *Ls/Sh* interbedded limestone and shale

To determine possible relationships between lithology and porosity, correspondence analysis was applied to lithologic data collected through petrographic analysis and point-counting (Table 3). Correspondence analysis provides a graphical display of attributes (lithology and porosity) and individual samples, where the distance between points is a measure of the similarity or correlation. A complete explanation of this method is present in a number of publications (e.g., Greenacre 1984; Davis 1986).
Groups of sample points characterize members of a specific family or individuals resulting from the same process, whereas groupings of attributes indicate similarity of behavior or correlation between attributes. Interpretation of correspondence factors is based on locating the attributes and sample end-members. All other points between the two end-members are considered mixtures of those end-members.
A graphical display of the quantitative information from Table 3 is shown in Fig. 5, where the eigenvalues have been adjusted to percentages. Within this data set the first factor accounts for 67% of the total variation and the second factor accounts for 18% of the total variation. The two attribute end-members on the factor 1 axis are dolomite and micrite, and this factor is the result of carbonate mineralogy (i.e., $MgCa(CO_3)_2$ vs $CaCO_3$). Samples that cluster near the dolomite end-member (100%) have the higher percentages of dolomite, whereas those samples located at the low end of the factor 1 axis are higher in micrite (Fig. 5). The two end-members for the factor 2 axis are sparite (coarsely crystalline calcite) and clay and represent overall grain/crystal size. These attributes and their associated samples plot away from the dolomite attribute.
Important with respect to porosity development in the Cmn is that the attribute porosity plots near the high end of the factor 1 axis, near the dolomite attribute, indicating a strong correspondence between dolomite and higher porosity (Fig. 5). Conversely, samples associated with micrite, sparite, and clay do not correspond with higher porosities. Thus, correspondence analysis reaffirms the petrographic observations that porosity is directly related to dedolomitization of the dolomitic facies in the Cmn.
In summary, the microporosity and mesoporosity within the different zones and lithofacies within those zones must by incorporated into hydrologic models of this aquifer. Microporosity and small mesoporosity that form the matrix porosity can be an important secondary source of contaminants into the fracture systems (e.g., Shevenell and others 1994). Matrix diffusion of possible contaminants from micro- and mesopores into fractures will differ considerably from one lithofacies or zone to another. Therefore, effects of matrix diffusion of contaminants within zone 6 will differ from the other Cmn zones due to the higher micro- and mesoporosity of zone 6.

Table 3
Petrographic analysis of the Maynardville Limestone. Data herein used in correspondence analysis (Fig . 5), except miscellaneous mineralogies: (*p*) pyrite; (*h*) hematite; (*g*) gypsum, vein filling; (*gl*) glauconite; (*b*) barite, lining vug

Sample number	Cmn			Composition (%)				Porosity	Misc.
	Well	Depth (m)	zone	Clay	Dolomite	Sparite	Micrite		
1	GW-135	223	6	1.3	97	0	0	1.6	0
2	GW-135	227	6	5.3	91	2.3	0	1.3	0
3	GW-135	234	6	1	88	0.6	0	10.3	0
4	GW-135	246	5	0	22.3	57	20	0.3	0.3 (p)
5	GW-135	249	5	26.6	30.3	22.6	19.6	0	0.6 (p)
6	GW-135	255	5	0.3	12	51.6	36	0	0
7	GW-135	269	4	0	16.6	49	34.3	0	0
8	GW-135	290	4	0	53.6	30.6	13.6	0	2.0 (p)
9	GW-135	307	3	2.6	16	47.3	34	0	0
10	GW-135	318	3	17.6	12	30.6	39.6	0	0
11	GW-135	345	2	2.6	11	35	51.3	0	0
12	GW-135	365	2	1	6.3	38.2	53.6	0.3	0.3 (p)
13	GW-137	40	3	11.3	1.6	21.6	65.3	0	0
14	GW-137	67	2	2.6	0	40.6	52	3	1.6 (h)
15	GW-138	132	6	2	78.6	4.3	0	15	0
16	GW-138	147	6	0.3	95.3	0	0	4.3	0
17	GW-138	164	6	0	67.6	1.3	30.9	0	0
18	GW-138	171	5	0	9.6	2.3	87.9	0	0
19	GW-138	173	5	0	36.6	49.3	13.6	0.3	0
20	GW-138	191	4	0	91	7.3	0	0	1.6 (p)
21	GW-138	201	4	0.3	6.3	63.6	29	0	0.3 (p)
22	GW-138	207	4	1.3	25.6	43.3	22.6	0	7.0 (g)
23	GW-138	216	4	0	87	8.3	1.3	0	3.3 (g)
24	GW-138	221	3	3	15	50.6	31.3	0	0
25	GW-138	239	3	2	35	51.9	11	0	0
26	GW-138	262	2	6.3	60	18.9	11	3	0.6 (gl; p)
27	GW-138	288	2	1.3	18	21.3	57.6	1.3	0.3 (b)

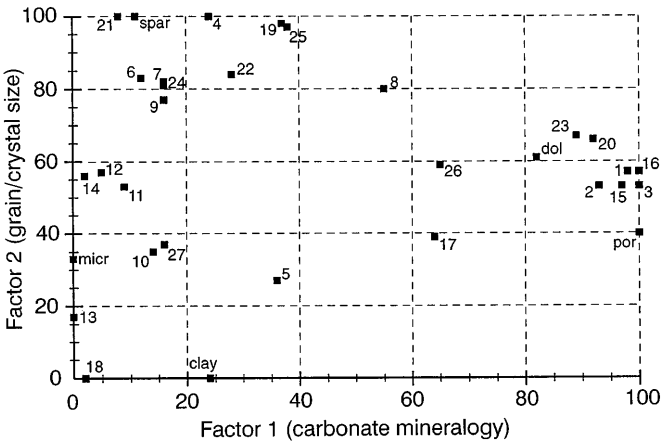

Fig. 5
Correspondence analysis plot of petrographic parameters (clay, dolomite, sparite, micrite, and porosity) for 27 samples. Data from Goldstrand and others (1995) and summarized in Table 3. Numbered squares refer to sample numbers shown in Table 3 (*por* porosity, *micr* micrite, *spar* sparite, *dol* dolomite)

Depth of karst formation

During drilling operations throughout BCV, numerous water producing intervals have been identified within the Cmn and Ccr. Of these water zones, 36% are identified as cavities, 32% are fractures, and 32% are identified as slow-flow water-producing intervals (Shevenell and Beauchamp 1994). The depth distribution of water zones encountered during drilling of 137 different wells which penetrated the Cmn (data from Jones and others 1992) were compiled. The Cmn zones encountered were not noted during drilling of the older wells which comprise 56% of the wells used in this analysis. Hence, the Cmn zone at particular depths in these wells was estimated by constructing the three-dimensional geology of BCV from data from wells shown in Fig. 3. The locations and depths of the older wells were interpolated into the three-dimensional geologic model to determine zone boundaries.

In addition, many of the wells in BCV were drilled to only very shallow depths. Of the 137 wells, 18 were drilled to depths <10 m, 41 to depths from 10 to 20 m, and 18 to depths between 20 and 30 m for a total of 56% of all wells. Because all of these wells are heavily biased toward the very shallow depths, the frequency of water zones at shallow depths would appear much larger than at deeper levels if these wells were considered in an anal-

ysis. Therefore, a subset of the data was selected such that all data from a total of 60 wells drilled to ≥30 m in all Cmn zones were included in order that more realistic comparisons between depths of 0 and 30 m could be made (Fig. 6).

In this figure, the subdivisions are identified as follows: 5 refers to that interval <5 m in depth, 10 identifies the interval 5–10 m in depth, etc. These data show that cavities are much more important than other water zones in the >10 to <20 m depth interval, with cavities decreasing with depth after 20 m and becoming less likely to be present than other water zones as depth increases. Some cavities have been noted at depths as great as 75 m, yet the vast majority (86%) are at depths <35 m. Below 35 m, other water zones (fractures and matrix porosity) are far more common. Note that of the 60 wells drilled below 30 m, 27 are from depths of 30–50 m, 16 between 50 and 100, 12 between 100 and 200, and only 5 between 200 and 434 m. Hence, the apparent decrease in water zones with depth below 50 m is largely reflecting the smaller data set at the deeper levels. Nevertheless, water zones dominate over cavities at all depths below approximately 25 m indicating conduit formation is strongly depth dependent when all Cmn zones are considered.

Although the data set is more limited, cavity frequency plots were also constructed within each individual Cmn zone to determine if there were specific depth dependencies within the zones and if differences between the zones could be identified. This evaluation is again restricted to all water zones at depths <30 m from wells which were drilled to a minimum depth of 30 m. Hence, all wells and water zones evaluated occur over the same, consistent depth interval in order to minimize introduction of bias into the data set. Between 6 and 11 wells in each Cmn zone were available for use, and insufficient data were available in this restricted depth interval for zone 3. In zones 2, 4, and 5, the greatest number of cavities occur in the 10- to 20-m depth interval, with cavity occurrence decreasing with depth thereafter. In addition, in these three zones, cavities are more abundant than water zones in the 10- to 20-m depth interval. Zone 2 is plotted in Fig. 7 as an example. In contrast, although there is a slightly higher frequency of cavities in zone 6 at shallower depths (10–20 m interval) compared to the deeper levels (>20–30 m), other types of water zones are consistently more common than cavities at all depth intervals considered (Fig. 8). This is in contrast to the other zones where cavities are more common than other water zones at the shallower depths, with the trend reversing as depth increases. The difference in the occurrence of water zones in zone 6 in comparison to the other zones is consistent with the porosity data which indicate microporosity and mesoporosity in the rock matrix are considerably higher in zone 6 than in the other Cmn zones. Hence, slower flowing water zones will be more important in zone 6. Table 4 summarizes the number of cavities and water

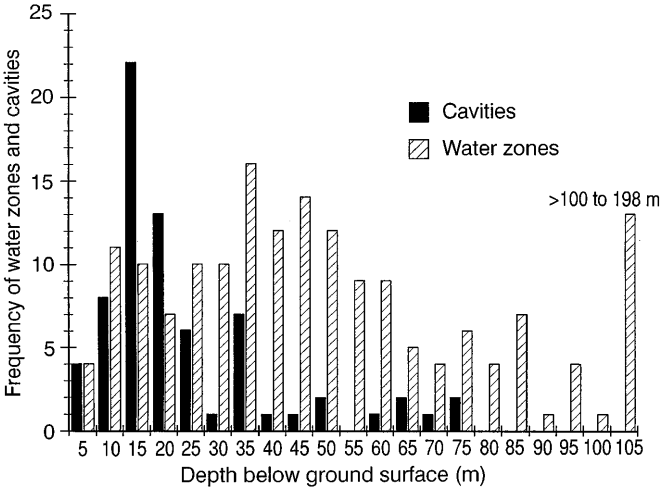

Fig. 6
Frequency of all water zones and cavities for all wells drilled in the Maynardville Limestone to depths >30 m

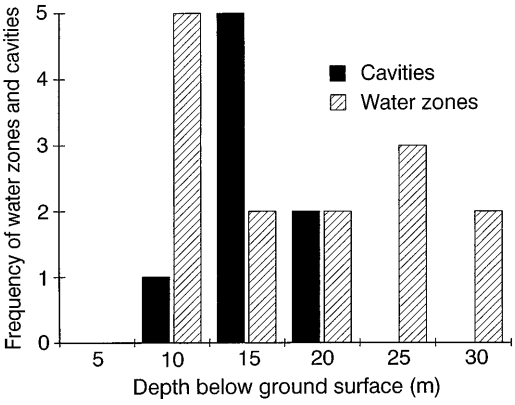

Fig. 7
Frequency of all water zones and cavities at depths between 0 and 30 m in Cmn zone 2. Data are from all wells drilled to depths greater than 30 m. Nine wells in zone 2 have noted 22 water zones between 0 and 30 m in wells drilled to >30 m in the Maynardville Limestone

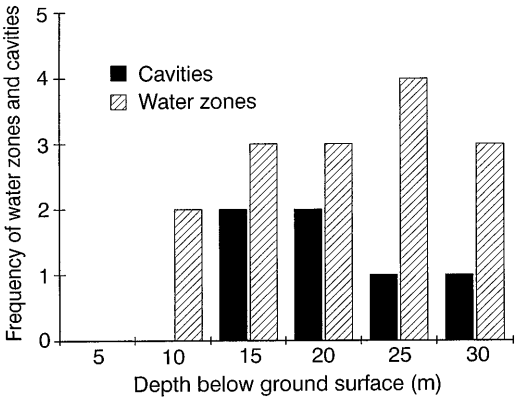

Fig. 8
Frequency of all water zones and cavities at depths between 0 and 30 m in Cmn zone 6. Data are from all wells drilled to depths greater than 30 m. Eleven wells in zone 6 have noted 21 water zones between 0 and 30 m in wells drilled to >30 m in the Maynardville Limestone

Table 4
Summary of the number of cavities and other water zones noted in wells drilled in the Maynardville Limestone. Three separate listings appear in the table: water zones at depths <30 m noted in wells drilled to depths of at least 30 m, water zones at depths <30 m from wells drilled to all depths, and all water zones noted in wells drilled to all depths. The columns are identified as follows: cavities/well = the total number of cavities divided by the number of wells penetrating the Cmn zone; water/well = the total number of other water zones noted divided by the number of wells penetrating the Cmn zone; total water/well = the total number of other water zones plus cavities noted divided by the number of wells penetrating the Cmn zone, and % cav = the percent of total water zones that are cavities

Cmn zone	No. of water zones	No. of cavities	Total no. of zones	No. of wells	Cavities/ well	Water/ well	Total water/ well	% Cav
Zone 2								
Wells >30m, water depths <30 m	14	8	22	9	0.89	1.56	2.44	36%
All wells, water depths <30 m	33	31	64	33	0.94	1.00	1.94	48%
All wells, all depths	45	36	81	37	0.97	1.22	2.19	44%
Zone 3								
Wells >30m, water depths <30 m	3	3	6	6	0.50	0.50	1.00	50%
All wells, water depths <30 m	9	15	24	15	1.00	0.60	1.60	63%
All wells, all depths	33	18	51	22	0.82	1.50	2.32	35%
Zone 4								
Wells >30m, water depths <30 m	7	10	17	7	1.43	1.00	2.43	59%
All wells, water depths <30 m	10	26	36	19	1.37	0.53	1.89	72%
All wells, all depths	33	26	59	32	0.81	1.03	1.84	44%
Zone 5								
Wells >30m, water depths <30 m	3	9	12	7	1.29	0.43	1.71	75%
All wells, water depths <30 m	5	10	15	10	1.00	0.50	1.50	67%
All wells, all depths	24	14	38	22	0.64	1.09	1.73	37%
Zone 6								
Wells >30 m, water depths <30 m	15	6	21	11	0.55	1.36	1.91	29%
All wells, water depths <30 m	27	21	48	24	0.88	1.13	2.00	44%
All wells, all depths	61	24	85	36	0.67	1.69	2.36	28%

zones encountered in each of the Cmn zones. Data are listed first for only the water zones <30 m in depth for wells drilled to >30 m in depth, second for wells and water zones at all depths, and third for water zones <30 m from all wells drilled to all depths. The tabulation for zone 3 at depths <30 m for wells >30 m deep is not reliable because of insufficient data. Well data compiled in Table 4 indicate that zone 6 contains fewer cavities relative to all other zones but generally has a larger number of slow-flow water intervals. These large-scale observations are reasonable when viewed in the context of the observed microporosity, mesoporosity, and vuggy-porosity values which are much higher in zone 6 than in any of the other Cmn zones. Hence, the microporosity and mesoporosity in the zone 6 rock matrix will be a more important control on groundwater flow and transport processes than within the lower Cmn zones. This is particularly true for the shallower intervals (10–20 m) where cavities are more dominant in the other Cmn zones. In the other Cmn zones, few slow-flowing water-producing intervals were noted and this is consistent with the generally lower microporosity to vuggy-porosity values measured in the matrix of these zones.

The number of water zones per well in zone 2 is slightly greater than the number of cavities per well for all three data sets listed in Table 4. Water zones encountered in zone 2 at depths <30 m occur exclusively within the valley floor where surface water and groundwater flow converges from the adjacent ridges. Hence, zone 2 at shallow depths is in one of the most active parts of the flow system, and greater amounts of water flow through this area allowing for greater dissolution and secondary porosity development than in most of the deeper levels of zone 2 for which porosity values were measured.

In Table 4, cavities per well are more common than other water zones per well in zones 3, 4, and 5 when only waters at depths <30 m are considered. However, when water zones at all depths are considered, other water zones are always more common than cavities. This reflects the fact that cavity occurrence decreases dramatically with depth in all Cmn zones.

In summary, cavities are much more important and common at the shallower depths than slow-flow water zones (Fig. 6). As depths increase, the frequency of cavities decreases substantially, and they are eventually absent, whereas the other types of slow-flow water zones increase significantly and dominate flow at depths below ≈ 35 m. Hence, large-scale secondary porosity development is strongly depth dependent, with decreasing development with increasing depth. This is in contrast to the general lack of depth dependency observed in the microporosity. Hence, the scale of observation (microporosity verses macroporosity) is critical in defining secondary porosity development.

Structural controls on karst development

Solution-enlarged fractures and fault planes are also important pathways for groundwater flow in BCV. Dissolution along fault planes in the Burial Grounds Waste Management Area provide conduits for groundwater flow to deeper levels. Cavities present along small-scale thrust faults, intersected during drilling, are connected to cavities intersected in another well, down dip, ≈ 33 m away (Goldstrand 1995).

Bedding-parallel and strike-parallel fractures are the most permeable sets of fractures in the area (Hatcher and others 1992). The frequency of fractures within the Cmn decreases with depth (Solomon and others 1992), and fracture spacing increases in thicker-bedded units (Hatcher and others 1992). Thus, solution-enlarged fractures will be more common at shallow depths than at deeper intervals within the Cmn, and will be more abundant in thinly bedded units.

Rapid fluid velocities can be expected along dip through cavities and fractures, and at shallow depths in all lithologies and at various angles to strike. Cavities encountered during drilling, and lithologic observations in core, indicate significant cavity development at shallow depths and significantly fewer karst features at greater depths. Significant quick flow can be expected throughout BCV, yet the directions of this flow may vary locally from site to site. In any hydrologic modelling of this aquifer, considerably higher hydraulic conductivities should be assigned to the shallow (<35 m) depths when modelling a large-scale problem. Smaller-scale problems should take into account the higher hydraulic conductivities expected along strike and dip directions.

Conclusions

Several important factors control porosity development in the Cmn and must be considered in hydrologic modelling of this part of the Knox aquifer. These factors are: (1) lithologic controls of secondary microporosity and mesoporosity, (2) depth below the ground surface related to the active groundwater system which influences cavity development, and (3) structural controls (solution-enlarged fractures and faults). Two interrelated diagenetic processes are the major controlling factors on development of microporosity to cm-scale vuggy porosity in the Cmn: dissolution of evaporite minerals and dedolomitization. Both of these diagenetic processes produce porosities as much as 10.3% in the dolomitic upper part of the Cmn to a depth of 230 m bgs. Microporosity to small mesoporosity formed by dedolomitization may also explain the decrease in porosity stratigraphically lower in the Cmn. The upper part of the Cmn (zone 6) has the highest porosities and consists mostly of dolostone and dolomitic limestone, whereas the middle and lower parts of the formation (zones 5 through 2) are dominantly limestone. Dedolomitization within the stromatolitic dolomite facies has produced the highest microporosity and mesoporosities within the Cmn. This feature is also evident from the drilling logs that show the upper Cmn has a greater percentage of slow-flowing water zones than in the lower Cmn due to the higher matrix porosities. Matrix porosities in zones 5 through 2 of the Cmn average between 0.8% and 0.5% but can be as much as 4.0%. Although, moldic porosity related to dedolomitization is locally common (e.g., dolomitized ooids in zone 5), much of the porosity is related to dissolution of carbonate mud interbeds. Also, within coarsely crystalline stromatolitic limestones, dissolution of intra-algal micrite produce thin, elongate solution zones. Oxidation and dissolution of pyrite also produces moldic porosity but is only of minor importance in parts of zone 2 located above approximately 60 m bgs.

Cavity development is strongly controlled by the depth of the active groundwater system in BCV and is generally independent of lithology. A large number of cavities have been intersected during drilling activities in nearly all zones of the Cmn in BCV at the shallow depths. Therefore, any of the Cmn zones within approximately 35 m of the ground surface are likely to contain cavities which allow rapid groundwater flow and contaminant transport (Goldstrand and Shevenell 1994).

Secondary megaporosity and cavities are strongly depth dependent and largely lithologically independent. Pre-existing fractures and bedding planes are more important in megaporosity and cavity development at shallow depths than they are to microporosity development at any depth. The reason for the differences in depth and lithologic dependencies can largely be attributed to the very active flow of groundwater through cavities and fractures at shallow depths in contrast to the more restricted flow in the matrix intervals at both the shallow and deeper levels.

Rapid fluid velocities can also be expected in various directions along the plane of dip in all lithologies and at various angles to strike in the Cmn. Hence, in any hydrologic modelling of this part of the Knox aquifer, considerably higher hydraulic conductivities should be assigned to the shallow (<35 m) depths when modelling a large-scale problem. Smaller-scale problems should take into account the higher hydraulic conductivities expected along strike and dip directions.

Acknowledgements This work was supported, in part, by subcontracts to the University of Nevada, Reno from Lockheed Martin Energy Systems, Inc. under the US Department of Energy's contract DE-AC05-84OR21400. The authors would like to thank RaNaye Dreier, Peter Lemiszki, Kevin Jago, and Craig Rightmire for their helpful discussions and suggestions and Laurie Menefee for help with porosity analysis. We wish to thank an anonymous reviewer for his/her helpful comments on this manuscript.

References

Back W, Hanshaw BB, Plummer LN, Rahn PH, Rightmire CT, Rubin M (1983) Process and rate of dedolomization: mass transfer and ^{14}C dating in a regional carbonate aquifer. Geol Soc Am Bull 94:1415–1429

Brown ET (ed) (1981) Rock characterization testing and monitoring. Pergamon Press, New York, pp 81–89

Choquette PW, Pray LC (1970) Geologic nomenclature and classification of porosity in sedimentary carbonates. Am Assoc Pet Geol Bull 54:207–250

Davis JC (1986) Statistics and data analysis in geology. Wiley, New York

Dreiss SJ (1984) Effects of lithology on solution development in carbonate aquifers. J Hydrol 70:295–308

Foreman JL, Walker KR, Weber LJ, Driese SG, Dreier RB (1991) Slope and basinal carbonate deposition in the Nolichucky Formation (Upper Cambrian) east Tennessee: effect of carbonate suppression by siliciclastic deposition on basin-margin lithologies. In: Lomando AJ and Harris PM (eds.), SEPM Core Workshop on mixed carbonate-siliciclastic sequences Spec Publ 15, Tulsa, Okla: Society of Economic Paleontologists and Mineralogists, pp 511–539

Geraghty and Miller Inc. (1985) Remedial alternative for Bear Creek Valley Waste Disposal Area. Oak Ridge Y-12 Plant Rep Y/SUB/85-00206C/3

Geraghty and Miller Inc. (1987) Monitor-well documentation report for the 1987 Drilling Program at the Y-12 Plant. Oak Ridge Y-12 Plant Rep Y/SUB/87-00206C/20

Geraghty and Miller Inc. (1990) Comprehensive groundwater monitoring plan for the Oak Ridge Y-12 Plant. Oak Ridge Y-12 Plant Rep Y/SUB/90-002066C/5

Goldstrand PM (1995) Stratigraphic variations and secondary porosity within the Maynardville Limestone in Bear Creek Valley. Oak Ridge Y-12 Plant Rep Y/TS-1093, pp 199

Goldstrand PM, Shevenell LA (1994) Lithologic controls on karst development and groundwater flow in the Copper Ridge Dolomite and Maynardville Limestone, Oak Ridge, Tennessee. Geol Soc Am Abstr Program 26:204

Goldstrand PM, Menefee LS, Dreier RB (1995) Porosity development in the Copper Ridge Dolomite and Maynardville Limestone, Bear Creek Valley and Chestnut Ridge, Tennessee. Oak Ridge Nat Lab Y-12 Rep Y/SUB95-SP912V/1, pp 49

Greenacre MJ (1984) Theory and application of correspondence analysis. Academic Press, Orlando

Hatcher Jr RD, Lemiszki PL, Dreier RB, Ketelle RH, Lee RR, Lietzke DA, McMaster WM, Foreman JL, Lee SY (1992) Status report on the geology of the Oak Ridge Reservation. Oak Ridge Nat Lab Rep ORNL/TM-12074, pp 244

Jones SB, Harrington BK, Field SM (1992) Updated subsurface data base for Bear Creek Valley, Chestnut Ridge, and parts of Bethel Valley on the U.S. Department of Energy Oak Ridge Reservation. Oak Ridge Y-12 Plant Rep Y/TS-881, pp 274

Ketelle RH, Huff DD (1984) Site characterization of the west Chestnut Ridge site. Oak Ridge Nat Lab Rep ORNL/TM-9229, pp 137

King HL, Haase CS (1987) Subsurface-controlled geological maps for the Y-12 Plant and adjacent areas of Bear Creek Valley. Oak Ridge Nat Lab Rep ORNL/TM-10112, pp 21

Rauch HW, White WB (1970) Lithologic controls on the development of solution porosity in carbonate aquifers. Water Res 6:1175–1192

Rothschild ER, Turner RR, Stow SH, Bogle MA, Hyder LK, Sealand OM, Wyrick JJ (1984) Investigation of subsurface mercury at the Oak Ridge Y-12 Plant. Oak Ridge Nat Lab Rep ORNL/TM-9092, pp 258

Saunders JA, Toran LE (1994) Evidence for dedolomitization and mixing in Paleozoic carbonates near Oak Ridge, Tennessee. Ground Water 32:207–214

Shevenell L (1996) Analysis of well hydrographs in a karst aquifer: Estimates of specific yields and continuum transmissivities. J Hydrol 174:331–356

Shevenell L, Dreier RB, Jago WK (1992) Summary of fiscal years 1991 and 1992 construction, hydrologic, and geolocical data obtained from the Maynardville Limestone Exit Pathway Monitoring Program. Oak Ridge Y-12 Plant Rep Y/TS-814, pp 144

Shevenell L, Beauchamp J (1994) Evaluation of cavity occurrence in the Maynardville Limestone and Copper Ridge Dolomite at the Y-12 Plant using logistic and general linear models. Oak Ridge Y-12 Plant Rep Y/TS-1022, pp 43

Shevenell LA, Moore GK, Dreier RB (1994) Contaminant spread and flushing in fractured rocks near Oak Ridge, Tennessee. Ground Water Monit Rem 14:120–129

Sledz JJ, Huff DD (1981) Computer model for determining fracture porosity and permeability in the Conasauga Group. Oak Ridge Nat Lab Rep ORNL/TM-7695

Solomon DK, Moore GK, Toran LE, Dreier RB, McMaster WM (1992) Status report, a hydrologic framework for the Oak Ridce Reservation. Oak Ridge Nat Lab Rep ORNL/TM-12026, pp 116

Weber Jr LJ (1988) Paleoenvironmental analysis and test of stratigraphic cyclicity in the Nolichucky Shale and Maynardville Limestone (Upper Cambrian) in central east Tennessee. Ph. D. thesis, University of Tennessee, Knoxville

Oak Ridge Reports can be purchased from NTIS (National Technical Information Service) U.S. Dept of Commerce, 5285 Port Royal Rd, Springfield, VA 22161 (1-800-553-6847) or through Interlibrary loan, Section Library, Environmental Sciences Division, Bldg 1505, Oak Ridge National Lab, Oak Ridge, TN 37831.